

Full paper / Mémoire

A structure–activity investigation of hemifluorinated bifunctional bolaamphiphiles designed for gene delivery

Mélanie Brunelle^b, Ange Polidori^{a,*}, Séverine Denoyelle^a, Anne-Sylvie Fabiano^a,
Pascal Y. Vuillaume^{b,1}, Sylvette Laurent-Lewandowski^b, Bernard Pucci^{a,*}

^a *Laboratoire de Chimie Biorganique et des Systèmes Moléculaires Vectoriels, Université d'Avignon et des pays du Vaucluse, 33 rue Louis Pasteur, 84000 Avignon, France*

^b *Université de Montréal, Faculté de Médecine Vétérinaire, 3200 rue Sicotte, Saint-Hyacinthe, Québec J2S 2M2, Canada*

Received 24 January 2008; accepted after revision 15 May 2008

Available online 14 November 2008

Abstract

A new series of dissymmetric hemifluorocarbon bolaamphiphiles were designed to investigate their main characteristics as a non-viral gene transfer carrier. The dissymmetric functionalization of diiodoperfluorooctane led to bolaamphiphile molecules composed of a partially fluorocarbon core end-capped with a glycoside and an ammonium salt. The physical–chemical results, cytotoxic effect, gene complexation and transfection efficiency were analyzed and functional relationships were addressed. The study clearly showed that the chemical structure of bolaamphiphiles influences the complexation with DNA, gene transfer, and cytotoxicity. Two different polar head groups (histidine and lysine) have been tested for their efficiency to complex DNA. The impact of the side chain of bolaamphiphile on the interaction with DNA was also investigated. Good transfection activity was demonstrated for partially fluorinated bolaamphiphile having lysine head group. Weak cell cytotoxicity, positive surface charge of bolaplexes, well-defined structure, and protection from the DNAses seem to be essential characteristics for efficient transfection. **To cite this article:** M. Brunelle et al., *C. R. Chimie* 12 (2009).

© 2008 Académie des sciences. Published by Elsevier Masson SAS. All rights reserved.

Résumé

L'étude porte sur les potentialités d'une nouvelle série d'agents amphiphiles dissymétriques hémifluorocarbonés dans le domaine de la transfection de gènes. La dissymétrisation fonctionnelle du diiodoperfluorooctane a permis d'accéder à des structures bolaamphiphiles dotées d'un cœur fluorocarboné et de terminaisons de type saccharidique et ammonium. Les propriétés physico-chimiques, le type de structure supramoléculaire qu'ils forment en milieu aqueux, leur impact sur l'aptitude à la complexation et à la transfection de gènes de l'ensemble de ces structures ont été précisés. Une activité de transfection non négligeable a pu être

* Corresponding authors.

E-mail addresses: ange.polidori@univ-avignon.fr (A. Polidori), bernard.pucci@univ-avignon.fr (B. Pucci).

¹ Present address: Conseil National de Recherches Canada, Institut des Matériaux Industriels, 75 Boulevard de Mortagne, Boucherville, Québec J4B 6Y4, Canada.

observée pour les bolaamphiphiles partiellement fluorés et dotés de tête polaire cationique de type lysine. *Pour citer cet article* : M. Brunelle et al., C. R. Chimie 12 (2009).

© 2008 Académie des sciences. Published by Elsevier Masson SAS. All rights reserved.

Keywords: Bolaamphiphile; Hemifluorinated surfactants; Gene transfer; Bolaplexes; Cell cytotoxicity; Cationic polar head

Mots-clés : Bolaamphiphile ; Surfactants hémifluorés ; Transfert de gènes ; Bolaplexes ; Cytotoxicité cellulaire ; Tête polaire cationique

1. Introduction

Synthetic cationic lipids are becoming acceptable alternatives to viruses as DNA carrier and transfection agents due to their low immunogenicity and higher cargo carrying capacity for gene therapy agents [1,2]. Furthermore, they can be readily prepared and handled. However, since the discovery of the (*N*-[1-(2,3-dioleoyloxy)propyl]-*N,N,N*-trimethylammonium chloride) (DOTMA) [3] and its *in vitro* transfection ability, a large array of molecules have been developed to improve the low transfection rates usually observed *in vivo* by using synthetic carriers [4–13]. This loss of activity is in part due to the extra- and intra-cellular barriers that have to be by-passed to induce the final gene expression [14]. These barriers may be broken through, if the carrier surface has been first functionalized by groups that allow them to escape the reticulum endothelial system (RES), aim at other target tissues in the liver or lungs and get through the cell membrane down to the cytoplasm. Each problem has its solution, but the accumulation of problems to be solved leads researchers to design more complex carriers, either by post-functionalizing the head groups on their outer surface or by using adequate formulations [15]. One approach that would both theoretically and simultaneously allow to complex DNA and to functionalize the surface carrier through membrane targeting, membrane crossing or invisibility agents consists in using dissymmetric bolaamphiphiles (Fig. 1).

Bolaamphiphiles are surfactants made of one or two hydrophobic chains linked by their ends to two polar groups providing them water solubility and amphiphilic properties [16]. They can self-organize as monolamellar membranes likely to close up as vesicles [17]. Assymmetric aggregation of those layers around the DNA might be expected by using a cationic polar head (dedicated to the complexation of nucleic acids) and a second non-ionic glycosylated polar head for instance. Cationic DNA carriers suffer from severe limitations to their use due to their rapid clearance from the blood together with their strong cytotoxicity

— particularly of a hepatic nature [18–24]. In that condition, one may assume that if the bolaplexes are endowed with a non-ionic outer surface, then their interactions with the RES, as well as their gene delivery efficiency and their cytotoxicity, would be reduced. Moreover, the application of an adapted formulation composed of bolaamphiphiles first functionalized with targeting or membrane crossing agents would improve the *in vivo* efficiency of these DNA carriers. A few papers describe the potentialities of this family of compounds in DNA vectorization technologies, but none of them studied the correlations between their structures, phase behaviours, and DNA complexation and transfection activities [25–32]. We have developed a new family of dissymmetric hemifluorinated bolaamphiphiles (Fig. 2) [33].

These compounds showed remarkable modularity which favours variations in a number of their structural subunits: (i) a cationic polar head derived from amino acids such as lysine or histidine to complex DNA by electrostatic interactions, (ii) a glycosylated non-ionic polar head made of galactosyl or lactobionamide units to ensure surface neutrality of the complex and the possible targeting of membrane cells bearing specific lectins (in particular hepatocytes membranes), [29] (iii) a hemifluorinated hydrophobic part linked to two polar caps through amide bounds. (Fig. 3).

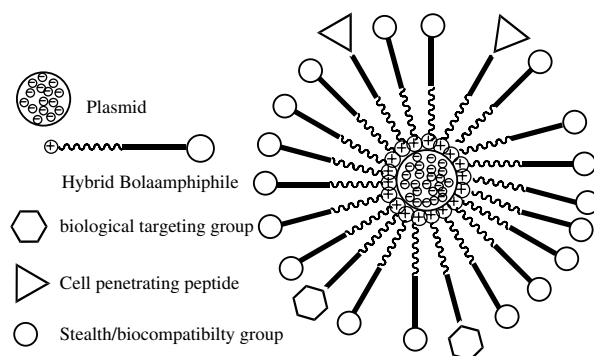


Fig. 1. Schematic representation of a polyfunctionalized bolaplex.

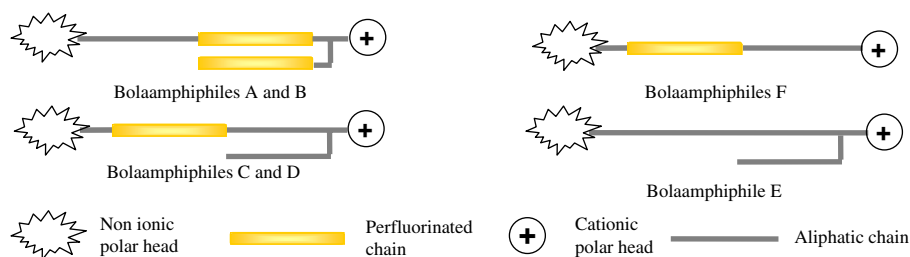


Fig. 2. Schematic representation of dissymmetric bolaamphiphiles.

The hydrophobic character can be reinforced by addition of a lateral chain grafted onto an amino acid. The hydro or perfluorinated nature of the side-link chain will be determined by the place of the

perfluorinated segment on the main chain. Because of the lipophobic character exhibited by fluorinated chains and in order to favour bolaplexes organization, the side chain must be located opposite

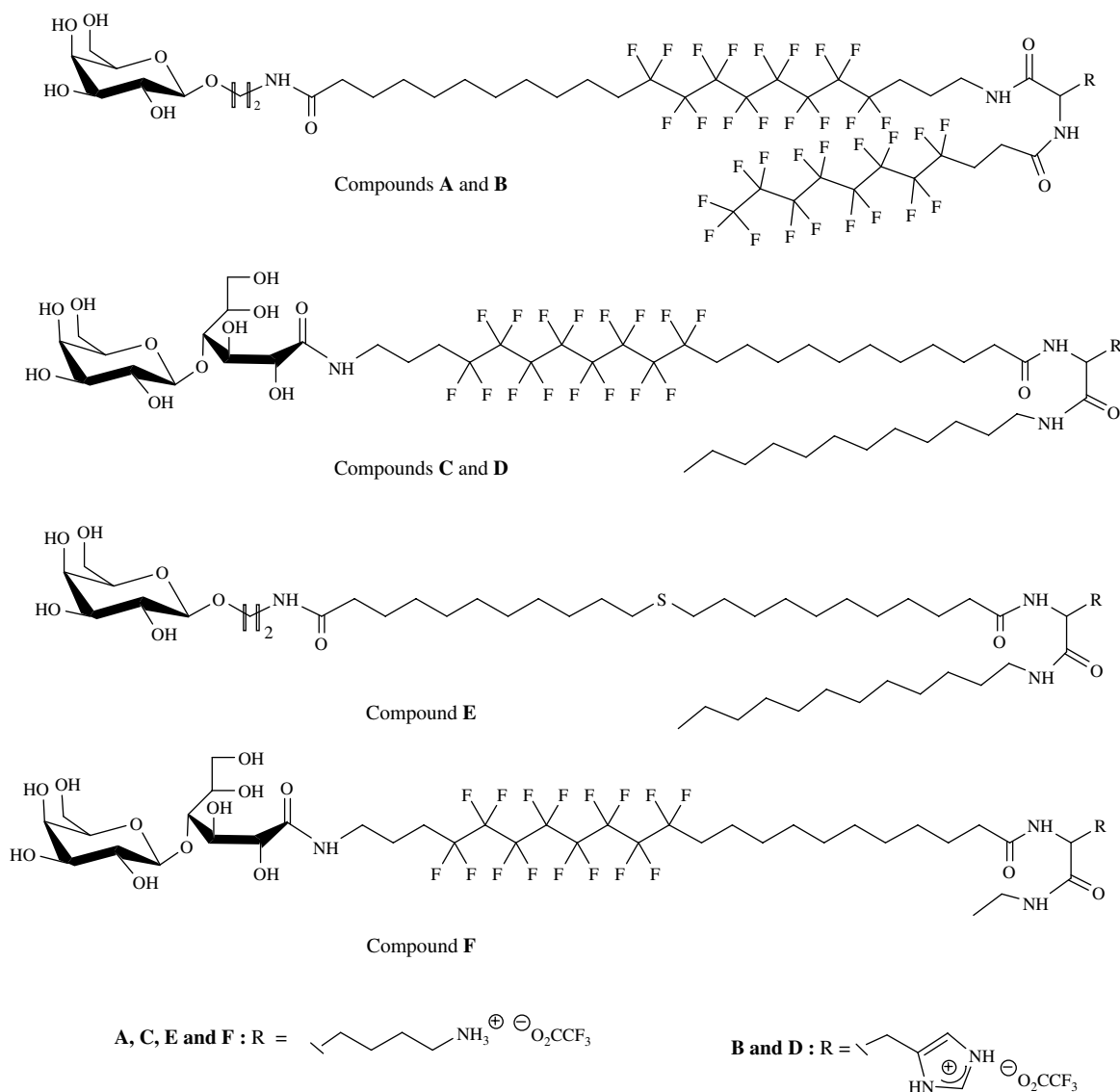


Fig. 3. Chemical structure of hybrid dissymmetric bolaamphiphiles A–F.

a hydrophobic segment of similar nature [34–37].

Inserting a perfluorinated segment is justified for several reasons. Because of their extremely high hydrophobic character, perfluorinated surfactants tend to form in aqueous solutions stable and compact self-organized membrane systems [34]. Thus, the fluorinated core may favour the stacking of the bolaplexes by increasing the cationic charge density around nucleic acids through hydrophobic interactions. Hui et al. have already shown that hemifluorinated surfactants could self-organize so as to form an asymmetric monolamellar membrane by bringing together all the fluorinated segments [37]. Thus, with such hemifluorinated bolaamphiphiles, the demixing of hydro and perfluorinated units should induce the formation of monolamellar membranes showing asymmetric polycationic and non-ionic surfaces. Such an asymmetry is then likely to favour a single level of DNA complexation, thus bringing about the formation of a neutral small-sized bolaplex. The aim of this paper is to demonstrate the impact of each of the five bolaamphiphiles' structural subunits on their associative behavior in aqueous milieu, their complexation efficiency of a DNA plasmid, the organization and physicochemistry of the bolaplexes formed, their cytotoxicity and their relative capacity to transfect DNA.

2. Experimental procedures

2.1. General procedure and materials

The synthesis of hemifluorinated and hydrocarbonated bolaamphiphiles **A–E** was described earlier [33]. All solvents were purchased from Acros Organics. CH_2Cl_2 was distilled from P_2O_5 and THF from sodium. Other solvents were used without further purification. All chemicals were purchased from Sigma–Aldrich or Acros Organics and were used without purification. Reactions were monitored by thin layer chromatography, using Merck precoated 60F₂₅₄ silica gel plates. Purifications were achieved by column chromatography over silica gel (Merck 60). Melting points were measured on an electrothermal apparatus and are uncorrected. ^1H NMR, ^{13}C NMR and ^{19}F spectra were recorded on a Bruker AC 250 spectrometer and processed using XWIN NMR (Bruker). Chemical shifts are given in parts per million relative to tetramethylsilane using the deuterium signal of the solvent as a heteronuclear reference for ^1H , ^{13}C and ^{19}F . Mass spectra were recorded on a APT III plus

Sciex apparatus. The branched polyethylenimine 25 kDa (PEI), fluorescent dye ethidium bromide (EtBr) and water (DNase/RNase-Free H_2O , molecular biology reagent) used for complexation experiments were obtained from Sigma–Aldrich (Oakville, ON). Plasmid pBudCE4.1/LacZ/CAT, Dulbecco's modified Eagle's medium (DMEM) and OPTI-MEM I and reduced serum medium were purchased from GIBCO Invitrogen (Burlington, ON). Foetal bovine serum (FBS) was from Medicorp (Montreal, PQ). The COS7 cell line (Simian virus 40-transformed kidney cells of an African green monkey) was from American Type Culture Collection (ATCC) (Valencia, CA). Cultureware was from Fisher Scientific (Montreal, PQ). The MTT cell proliferation kit [3-(4,5-dimethylthiazol-2-yl)-2,5-diphenyltetrazolium] and the β -GAL ELISA kit were purchased from Roche Diagnostics GmbH (Laval, PQ). RQ1 RNase-Free DNase was from Promega (Madison, WI). 1,2-Dioleoyl-*sn*-glycero-3-phosphoethanolamine (DOPE) was from Avanti Polar Lipids, Inc. (Alabaster, AL).

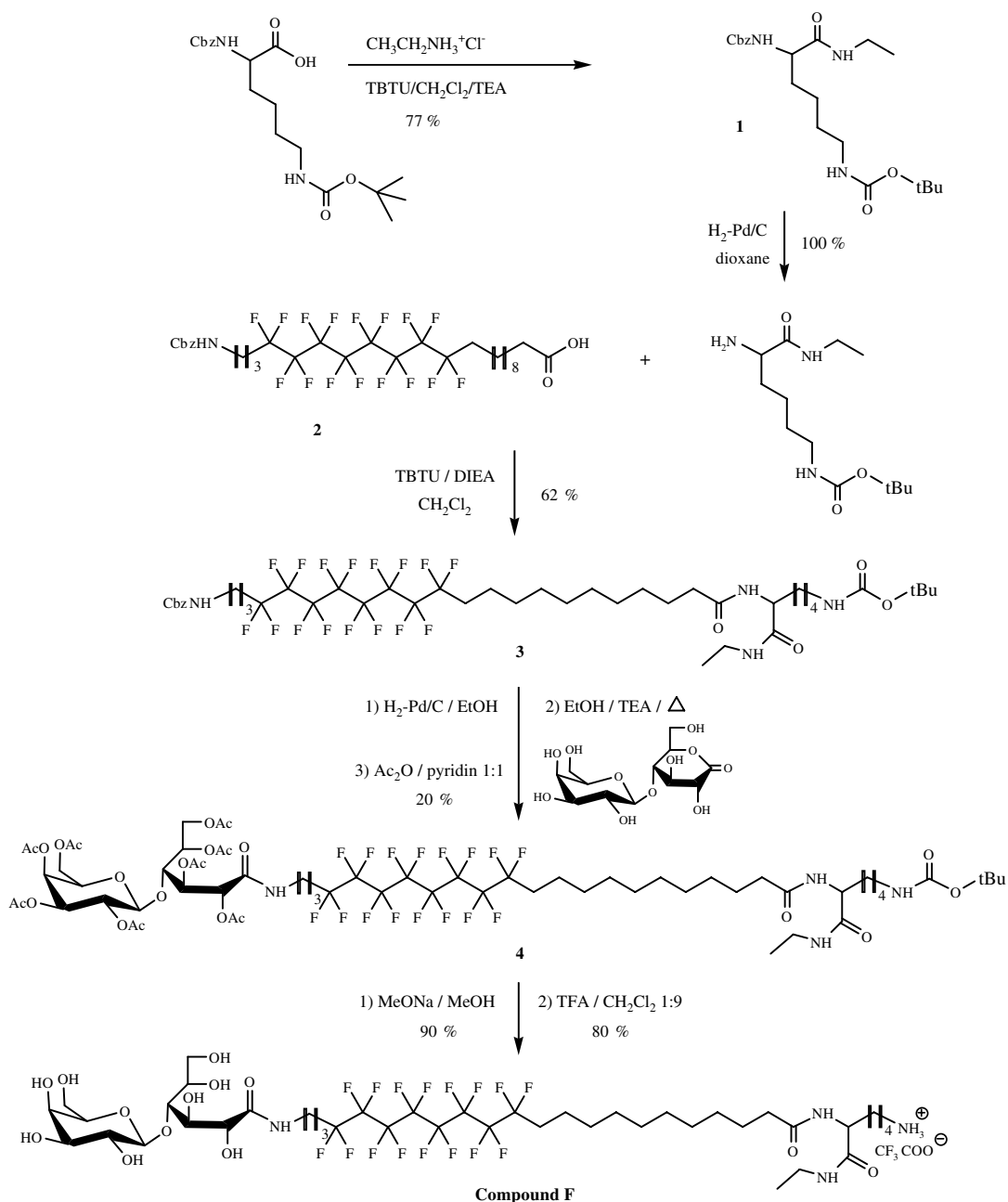
2.2. Synthesis

Hemifluorinated bolaamphiphile **F** was synthesized according to **Scheme 1** with compound **2** described earlier [33] as starting material, following a convergent synthetic pathway.

In a first sequence, *Z*-(N^{ϵ} -Boc)lysine was treated with ethylamine hydrochloride in the presence of *O*-(Benzotriazol-1-yl)-*N,N,N',N'*-tetramethyluronium tetrafluoroborate (TBTU) as coupling reagent to give compound **1** in good yield (77%). After removal of the α -amino protective group (hydrogenolysis in the presence of palladium on charcoal), the resulting amine was coupled with compound **2** [33] in the presence of TBTU to provide derivative **3** in 62% yield. Hydrogenolysis of the benzyloxycarbonyl group allowed condensation with lactobionolactone in boiling methanol with triethylamine. To carefully purify this compound through silica gel column chromatography, the sugar residue was acetylated with an acetic anhydride–pyridine mixture to give protected bolaamphiphile **4**. In a final sequence, removal of the acetyl groups with sodium methoxide and the Boc amino acid protecting group with TFA resulted in final bolaamphiphile **F**.

2.2.1. Synthesis of *N* $^{\alpha}$ -benzyloxycarbonyl-*N* $^{\epsilon}$ -*t*-butyloxycarbonyl-*N*-ethyl lysinamide **1**

In a sealed flask, *Z*-Lys(Boc)OH (1 g, 2.63 mmol), ethylamine hydrochloride (0.322 g, 3.95 mmol) and

Scheme 1. Synthetic pathway to bolaamphiphile **F**.

TBTU reagent (1.27 g, 3.95 mmol) were dissolved in 15 mL of freshly distilled CH_2Cl_2 under argon. The pH of the solution was raised with TEA (pH 8–9). After stirring for 16 h at room temperature, the solvent was removed *in vacuo* and the crude product was purified by flash chromatography on silica gel (AcOEt–cHex 4:6) to yield 0.830 g (2.04 mmol, 77%) of racemic compound **1** as a white solid. R_f : 0.5 (AcOEt–cHex

5:5 (v/v)), mp: 117.9–119.5 °C. ^1H NMR (CDCl_3 , 250 MHz): δ 1.10 (3H, t, CH_3 , $J^3 = 7.17$ Hz), 1.29–1.47 (11H, m, $\text{CH}-\text{CH}_2-\text{CH}_2$, $\text{C}(\text{CH}_3)_3$), 1.61 (2H, m, $\text{CH}_2-\text{CH}_2-\text{NH}(\text{Boc})$), 1.80 (2H, m, $\text{CH}-\text{CH}_2$), 3.20 (2H, m, $\text{NH}-\text{CH}_2-\text{CH}_3$), 3.24 (2H, m, $\text{CH}_2-\text{NH}(\text{Boc})$), 4.6 (1H, m, $\text{CH}-\text{CH}_2$), 4.80 (1H, s, NH), 5.02 (2H, s, $\text{CH}_2-\Phi$), 5.86 (1H, s, NH), 6.59 (1H, s, NH), 7.35 (5H, s, CH_{arom}). ^{13}C NMR (CDCl_3 ,

62.86 MHz): δ 14.7 (CH₃), 22.5 (CH–CH₂–CH₂), 28.4 (C(CH₃)₃), 29.6 (CH₂–CH₂–NH(Boc)), 32.2 (CH–CH₂), 34.4 (NH–CH₂–CH₃), 39.9 (CH₂–NH(Boc)), 54.9 (CH–CH₂), 66.9 (CH₂– Φ), 79.1 (C(CH₃)₃), 128.0–128.5 (CH_{arom.}), 136.2 (C_{arom.}), 156.3–156.4 (2HN–CO–O), 171.1 (CH–CO–NH).

2.2.2. Synthesis of *N* ^{α} -[20-(*N*-benzyloxycarbonyl)amino-12,12,13,13,14,14,15,15,16,16,17,17 dodecafluoro-eicosanoyl]amido-*N* ^{ϵ} -*t*-butyloxycarbonyl-*N*-ethyl lysinamide **3**

Compound **1** (245 mg, 0.602 mmol) was dissolved in 10 mL of dioxane. The solution was stirred and cooled to 0 °C and palladium on charcoal (36 mg, 60 mg mmol⁻¹) was added portion wise. The mixture was stirred under hydrogen pressure (8 bar) for 6 h at room temperature and was then filtered over Celite. The solvent was next removed *in vacuo*. The crude product (164 mg, 0.602 mmol) was dissolved in 5 mL of freshly distilled CH₂Cl₂ under argon. Compound **2** [33] (360 mg, 0.463 mmol) and TBTU (193 mg, 0.602 mmol) were then added. The pH of the mixture was adjusted to 8 with DIEA. After stirring for 16 h under argon at room temperature, the solvent was removed *in vacuo* and the crude product was purified by flash chromatography on silica gel (AcOEt–cHex 7:3) to yield compound **3** (296 mg, 0.287 mmol, 62%). *R*_f: 0.58 (AcOEt–cHex 5:5). ¹H NMR (CDCl₃, 250 MHz): δ 1.14 (3H, t, CH₃, *J*³ = 7.24 Hz), 1.25–1.38 (14H, m, CH₂ linear chain, CH–CH₂–CH₂), 1.45 (9H, s, C(CH₃)₃), 1.48–1.61 (8H, m, CH₂–CH₂–NH(Boc), 2CF₂–CH₂–CH₂, CH₂–CH₂–CO–NH), 1.84 (2H, m, CH–CH₂), 1.99–2.24 (6H, m, 2CH₂–CF₂, CH₂–CO–NH–CH), 3.11 (2H, m, CH₃–CH₂–NH–CO), 3.30 (4H, m, CH₂–NH(Boc), (Z)NH–CH₂), 4.12 (1H, td, CH–CH₂, *J*³ = 6.64 Hz, *J*³ = 7.50 Hz), 4.75 (1H, s, NH), 5.03 (1H, s, NH), 5.12 (2H, s, CH₂– Φ), 6.50 (1H, d, NH–CH–CH₂, *J*³ = 7.59 Hz), 6.67 (1H, s, NH), 7.37 (5H, s, CH_{arom.}). ¹³C NMR (CDCl₃, 62.86 MHz): δ 14.6 (CH₃), 20.1–29.6 (CH₂ linear chain, C(CH₃)₃, NH–CH–CH₂–CH₂–CF₂), 30.9 (2CH₂–CF₂), 32.1 (CH–CH₂), 34.4 (NH–CH₂–CH₃), 36.5 (CH₂–CO–NH), 40.0–40.1 (CH₂–NH(Boc), CH₂–NH(Z)), 52.8 (CH–CH₂), 66.9 (CH₂– Φ), 79.1 (C(CH₃)₃), 106.9–121.4 (CF₂), 128.1–128.6 (CH_{arom.}), 136.4 (C_{arom.}), 156.2–156.5 (2NH–CO–O), 171.6–173.4 (CH–CO–NH, CO–NH–CH). ¹⁹F NMR (CDCl₃, 235.19 MHz): δ –114.07 to –114.32 (4F, d, 2CH₂–CF₂), –121.79 (8F, m, 4CF₂), –123.48 (4F, s, 2CF₂).

2.2.3. Synthesis of *N* ^{α} -[20-(*N*-lactobionocarbonyl)amino-12,12,13,13,14,14,15,15,16,16,17,17 dodecafluoro-eicosanoyl]amido-*N* ^{ϵ} -*t*-butyloxycarbonyl-*N*-ethyl lysinamide **4**

Compound **3** (175 mg, 0.170 mmol) was dissolved in 10 mL of ethanol. The solution was stirred and cooled to 0 °C and palladium on charcoal (10 mg, 60 mg mmol⁻¹) was added portion wise. The mixture was stirred under hydrogen pressure (8 bar) for 48 h at room temperature. The mixture was filtered over Celite and the solvent was removed *in vacuo* to yield the amine (148 mg, 0.165 mmol, 97%) as a white powder. At the same time, lactobionic acid (89 mg, 0.248 mmol) was dissolved in 20 mL of a 1:1 toluene–methanol mixture. A few drops of TFA were added and the solvents were removed *in vacuo*. The operation was repeated twice and the lactobionolactone obtained was added to the previous amino compound. Then, the mixture was dissolved in 20 mL of distilled ethanol under argon, the pH of the solution was raised with TEA to pH 8–9 and the mixture was refluxed under argon for 16 h. After removing the solvent *in vacuo*, 20 mL of a mixture of 1:1 acetic anhydride–pyridine were added. The reaction was stirred for 12 h at room temperature. The mixture was poured into a cooled 1 M HCl solution and the solution was extracted with ethyl acetate. The organic layer was washed with a saturated NaHCO₃ solution, then with brine and dried over sodium sulfate. The solvent was removed *in vacuo* and the crude product was purified by flash chromatography on silica gel (AcOEt–cHex 7:3 to AcOEt–cHex 9:1) to yield the fully protected bolaamphiphile **4** (54 mg, 0.034 mmol, 20%). *R*_f: 0.4 (AcOEt), [α]_D²⁰: +5.16° (*c* 1, CH₂Cl₂). ¹H NMR (CDCl₃, 250 MHz): δ 1.13 (3H, t, CH₃, *J*³ = 7.25 Hz), 1.25–1.37 (14H, m, CH₂ linear chain, CH–CH₂–CH₂), 1.44 (9H, s, C(CH₃)₃), 1.51–1.68 (8H, m, CH₂–CH₂–NH(Boc), 2CF₂–CH₂–CH₂, CH₂–CH₂–CO–NH), 1.75–2.24 (32H, m, CH–CH₂, 8CO–CH₃, 2CH₂–CF₂, CH₂–CO–NH), 3.11 (2H, m, CH₃–CH₂–NH), 3.18–3.32 (4H, m, CH₂–NH(Boc), NH–CH₂–(CH₂)₂–CF₂), 3.93–4.18 (4H, m, CH₅(^{5'}), CH₂(^{6'}), CH₆(^{6'})), 4.30–4.41 (2H, m, CH–CH₂, CH₄(^{4'})), 4.55–4.67 (1H, m, CH₆(^{6'})), 4.70 (1H, d, CH₁(^{1'}), *J*³ = 7.87 Hz), 4.89 (1H, m, NH), 4.92–5.22 (3H, m, CH₂(^{2'}), CH₃(^{3'}), CH₅(^{5'})), 5.39 (1H, m, CH₄(^{4'})), 5.54–5.58 (2H, m, CH₂(^{2'}), CH₃(^{3'})), 6.41–6.46 (2H, m, NH), 6.60 (1H, m, NH). ¹³C NMR (CDCl₃, 62.86 MHz): δ 14.6 (CH₃), 20.5–29.6 (CH₂ linear chain, CH–CH₂–CH₂–CH₂, C(CH₃)₃, NH–CH₂–CH₂–CH₂–CF₂, CH₂–CF₂, CO–CH₃), 32.2 (CH–CH₂), 34.4 (NH–CH₂–CH₃), 36.5 (CH₂–CO–NH), 37.9 (NH–CH₂–(CH₂)₂–CF₂),

39.4 (CH₂–NH(Boc)), 52.8 (CH–CH₂), 60.9 (CH_{2(6')}), 61.6 (CH₂₍₆₎), 66.8–71.6 (CH₍₂₎, CH₍₃₎, CH₍₅₎, CH_(2'), CH_(3'), CH_(4'), CH_(5')), 77.4 (CH₍₄₎), 79.1 (C(CH₃)₃), 101.7 (CH_(1')), 111.2–121.4 (CF₂), 156.2 (NH–CO–O), 167.4–173.2 (3CO–NH, CO–CH₃). ¹⁹F NMR (CDCl₃, 235.19 MHz): δ –114.06 to –114.35 (4F, d, 2CH₂–CF₂), –121.81 (8F, m, 4CF₂), –123.55 (4F, s, 2CF₂).

2.2.4. Synthesis of N^α-[20-(N-lactobionocarbonyl) amino-12,12,13,13,14,14,15,15,16,16,17,17 dodecafluoro-eicosanoyl]amido-N^ε-ammonium trifluoroacetate-N-ethyl lysinamide **F**

Compound **4** (50 mg, 0.0315 mmol) was dissolved in 10 mL of freshly distilled methanol. A catalytic amount of sodium methoxide was added. After stirring for 12 h, IRC50 ion exchange resin (1 g) was added. After 10 min the mixture was filtered. The solvent was removed *in vacuo* and the crude product was purified by size exclusion chromatography using Sephadex LH20 (MeOH) to yield deacetylated compound **F** as a white powder (34.4 mg, 0.0284 mmol, 90%). Then, this compound was dissolved in 9 mL of freshly distilled CH₂Cl₂. One milliliter of TFA was added dropwise. After stirring for 48 h at room temperature, the solvents were removed *in vacuo*. The crude product was dissolved in diethyl ether and the solvent was removed *in vacuo*. The operation was repeated twice. Lastly, the crude product was purified by size exclusion chromatography using Sephadex LH20 (MeOH) to yield compound **F** as a white powder (28.3 mg, 0.0227 mmol, 80%). mp_(dec): 64–75.5 °C. ¹H NMR (CD₃OD, 250 MHz): δ 1.13 (3H, t, CH₃, J³ = 7.23 Hz), 1.31–1.46 (14H, m, CH₂ linear chain, CH–CH₂–CH₂), 1.62–1.73 (8H, m, CH₂–CH₂–NH₃⁺, 2CF₂–CH₂–CH₂, CH₂–CH₂–CO–NH), 1.84 (2H, m, CH–CH₂), 2.15–2.30 (6H, m, 2CH₂–CF₂, CH₂–CO–NH), 2.94 (2H, m, CH₃–CH₂–NH), 3.21–3.96 (14H, m, CH₂–NH₃⁺, NH–CH₂–(CH₂)₂–CF₂, CH₍₄₎, CH₍₅₎, CH₂₍₆₎, CH_(2'), CH_(3'), CH_(4'), CH_(5'), CH_{2(6')}), 4.29–4.53 (4H, m, CH–CH₂, CH₍₂₎, CH₍₃₎, CH_(1')), 8.05 (2H, m, NH). ¹³C NMR (CD₃OD, 62.86 MHz): δ 13.4 (CH₃), 19.9–31.2 (CH₂ linear chain, CH–CH₂–CH₂–CH₂, NH–CH–CH₂–CH₂–CF₂, CH₂–CF₂, CH–CH₂), 33.9 (NH–CH₂–CH₃), 35.4 (CH₂–CO–NH), 37.2 (NH–CH₂–(CH₂)₂–CF₂), 39.5 (CH₂–NH₃⁺), 53.0 (CH–CH₂), 61.0 (CH_{2(6')}), 62.4 (CH₂₍₆₎), 69.0–75.8 (CH₍₂₎, CH₍₃₎, CH₍₅₎, CH_(2'), CH_(3'), CH_(4'), CH_(5')), 81.9 (CH₍₄₎), 104.4 (CH_(1')), 106.8–122.9 (CF₂), 172.5, 174.1, 175.0 (3CO–NH). ¹⁹F NMR (CD₃OD, 235.19 MHz): δ –76.75 (3F, s, [–]O₂C–CF₃), –115.29 (4F, s, 2CH₂–CF₂), –122.77 (8F, m, 4CF₂), –124.47 (4F, s, 2CF₂). (ESI–MS): [M + H⁺]⁺ m/z = 1139.7 (without CF₃COO[–]), [M + Na⁺]⁺ m/z = 1161.7 (without CF₃COO[–]).

2.3. Preparation of bola/DNA complexes

Bolaamphiphiles (10 mg) were dissolved in methanol in a round-bottomed flask (typically 50 mL). Organic solvent was removed under reduced pressure (rotary evaporator) giving a thin-lipid film that was dried *in vacuo*. Then DNase free water (2 mL) was added to hydrate the thin-lipid film. The mixture was mixed–vortexed for 5 min and then sonicated for 2 h in a sonication bath (ultrasonic Branson 3510 bath) at 60 °C. Plasmid pBudCE4.1/lacZ/CAT (8433 bp) encoding β-galactosidase under the control of the CMV promoter was used for all the experiments reported in this paper and produced as described elsewhere [38]. Bolaplexes were prepared at different electrostatic charge ratios (N/P) at a final DNA concentration of 10 μg mL^{–1} in Sigma DNase/RNase-Free H₂O. In each case, the appropriate amount of bola diluted in water (0.5 mg mL^{–1}) was added in a final volume of 500 μL of water to obtain the appropriate concentration for the desired N/P ratios. N/P ratios were calculated from the number of the electrostatic charges present in bola (terminal NH₂ groups) and DNA (phosphate groups). The bola solution was gradually added to the 500 μL of DNA solution (20 μg mL^{–1}), with a vortex time of 30 s between each addition. After complete addition, the resulting solution (containing **A**, **B**, **C**, **D**, **E** or **F** bolaplexes) was stirred for 30 s and incubated at room temperature for 15 min.

2.4. Preparation of C-bolaplex containing DOPE

Bola **C** was mixed with DOPE in a round-bottomed flask at a molar ratio of 1:1 and diluted in methanol. The mixture was then dried, vacuum desiccated and resuspended in water at a final bola **C** concentration of 0.5 mg mL^{–1} before being vortexed and sonicated for 1 h at 60 °C in a sonication bath. The resulting solution (bola **C**/DOPE) was used for the preparation of bolaplexes in exactly the same way as the other bola solutions.

2.5. Agarose gel electrophoresis retardation assays

Interactions between plasmid DNA and bola dispersions were investigated by electrophoresis on agarose gels. Bolaplexes were prepared at different N/P ratios with bolaamphiphiles **A**–**F** as described above. The naked DNA solution, as control, or 40 μL of bolaplexes containing each 400 ng of DNA were mixed with bromophenol blue in glycerol. They were then subjected to electrophoresis on a 0.8% (w/v)

agarose gel [Tris-acetate–EDTA buffer (TAE) pH 8.5, 90 V, 90 min]. DNA bands were visualized by UV illumination after coloration with ethidium bromide ($0.5 \mu\text{g mL}^{-1}$) for 30 min. The complete complex formation resulted in retardation of the DNA in the loading well of the gel.

2.6. Ethidium bromide exclusion assay

Fluorescence studies with EtBr fluorescent dye were carried out at 24°C with a Fluoromax-2, Horiba, Jobin Yvon Spex, fluorescence spectrometer (1 cm path length; quartz cell; slit width 5 nm; xenon lamp 150 W). As reported elsewhere, λ excitation and λ emission were set at 520 and 597 nm, respectively. In the displacement assay, DNA was first mixed and vortexed with fluorescent dye EtBr, at final concentrations of 20 and 400 ng mL^{-1} , respectively, as suggested elsewhere [41]. Dye-labeled DNA was allowed to equilibrate for 5 min in the dark after which complexes of dye-labeled DNA with bolaamphiphiles were formed by adding the bola solutions at the desired *N/P* ratios with an equal volume of dye-labeled DNA solution (final concentrations of DNA $10 \mu\text{g mL}^{-1}$). The bolaplexes were allowed to equilibrate in the dark for 15 min before fluorescence measurement. Controls were performed with PEI complexes using similar *N/P* ratios. The relative fluorescence intensity of the resulting complex was expressed by the following equation: relative fluorescence intensity (I) = $F_{\text{obs}} - F_0 / F_{\text{DNA}} - F_0$; where F_{obs} is the fluorescence intensity of the bolaplexes, F_0 is the fluorescence intensity of the dye in water alone, and F_{DNA} is the dye-labeled DNA in the absence of bola. Experiments were repeated three times.

2.7. Stability of bolaplexes to DNase I

The stability of the bolaplexes to the action of DNase I was analyzed with respect to the *N/P* ratio and time. Naked DNA used as positive control and bolaplexes were incubated with DNase I (1 Unit by μg of DNA) in the presence of $1 \times$ DNase I reaction buffer. The reaction was carried out at 37°C and the aliquots for analysis were taken at 0, 10 and 30 min. For inhibition of the enzymatic reaction, incubation during 10 min at 60°C with 0.5 M EDTA (for a final concentration of 50 mM) was adopted. Finally, to favour the decomplexation between the DNA and the bola, a 10% SDS solution was added (for a final 2% concentration). DNA degradation was observed following an agarose gel

electrophoresis of the resulting solution. Experiments were repeated three times. It has to be noted that bolaplexes containing $10 \mu\text{g}$ pBudCE4.1/LacZ/CAT were also incubated only in the presence of buffers utilized (data not shown), as control, to verify the impact of the buffers on the integrity of complexation.

2.8. Size distribution and zeta (ζ) potential measurements

Size and surface charges (ζ -potential) of bolaplexes prepared at different *N/P* ratios in water were measured by quasi-elastic light scattering (QELS) using a Zetasizer (Malvern, NanoZS ZEN3600). Size measurement followed by the ζ -potential measurement (calculated using the Schmoluchowsky approximation) were performed on each freshly prepared bolaplex (see Section 2.3) using disposable cells (Folded capillary cell DTS 1060). The instrument was equipped with a monochromatic coherent helium neon laser (633 nm) as a light source. The scattered light was recorded at an angle of 173° , and the analysis of the autocorrelation function was performed automatically to yield diffusion coefficients, D_T , taking the values 1.33 and 25°C for refractive index and temperature, respectively. Volume distributions of the bolaplex size were given according to the hydrodynamic diameter using multimodal distribution.

2.9. Transmission electron microscopy (TEM)

Bolaamphiphiles **A–F** and the corresponding bolaplexes were deposited on a 150-mesh copper grid covered with Formvar and were then negatively stained with a droplet of 1% aqueous uranyl acetate (without pH adjustment and filtered on $0.22 \mu\text{m}$). The excess of colorant was gently wicked off with filter paper and the grid was air-dried. The observations were performed on a Philips EM 410 at 80 kV acceleration voltage and $3000\text{--}250,000\times$ magnification.

2.10. In vitro transfection experiments

COS7 cells were used for transfection and cell viability tests. Plasmid pBudCE4.1/lacZ/CAT (8433 bp) was used for the experiment. Cells were grown before in 6-well plates for 24 h at an initial seeding density of 2.7×10^5 per well at 37°C using DMEM containing L-glutamine, 10% FBS and 1% gentamicin. Cells were transfected at 90% confluence. Just before the transfection experiment, the medium

was removed and the cells were washed twice with phosphate buffered saline (PBS). Transfections were performed in a serum-free solution: 1 mL of OPTI-MEM I serum-free medium was added before the addition of the bolaplex solution (500 μ L, equivalent to 5 μ g of DNA/well). Serum-free transfection mixtures were incubated for 4 h after which the medium was replaced with complete medium for 20 h. Transfection studies were also performed in the presence of 2.0% serum and with the help of a co-lipid (DOPE). For transfection experiments in the presence of serum, 1 mL of complete medium containing 2.0% of serum (without antibiotics) was used instead of the OPTI-MEM I serum-free medium. For transfection in the presence of bolaamphiphile C/DOPE, the method employed for the traditional complexes was used. After total incubation for 24 h, cells were harvested, as described in the available commercial kit, after which β -galactosidase concentration was measured. Results were expressed as picograms of β -galactosidase per μ g of total protein previously determined by the BCA (Bicinchonic acid) assay (Pierce). Controls were performed with the naked DNA plasmid (5 μ g of DNA) as negative control or with PEI using a PEI-DNA *N/P* ratio of 10, *i.e.*, corresponding to optimal conditions defined elsewhere, as positive control [42]. Transfection experiments were repeated three times.

2.11. Cytotoxicity assay

The cytotoxic effect of bolaamphiphiles or bolaplexes was evaluated by measuring the viability of the cells treated. The metabolic activity of viable COS7 cells was measured using the MTT Cell Proliferation Assay kit 24 h after incubation of the cells with varying bola concentrations corresponding to the quantity of bola(amphiphile)s used at the different *N/P* ratios tested in the transfection experiment or with the bolaplexes at the indicated *N/P* ratio. Cells were firstly grown in 96-well plates 24 h before the experiment at an initial seeding density of 1.9×10^4 cells/well in 100 μ L of complete medium. The medium was removed and replaced by the bola solution prepared in the OPTI-MEM I. Cells treated were incubated for 24 h and then tested for their metabolic activity. Ten microliters of MTT reagent (10% v/v; final concentration 0.5 mg mL⁻¹) was added to each well. After 4 h of incubation at 37 °C, the purple insoluble salt was dissolved by adding 100 μ L of solubilization solution. The plates were incubated in the dark at 37 °C for 24 h. Absorbance was measured at 550 nm using a reference wavelength of 650 nm. The results were expressed as

a relative percentage of cell viability related to the control (naked DNA-treated cells). The cell viability of cells treated with naked DNA only was used as 100% of cell viability. Cell viability (relative %) = $(OD_{(550-650)} \text{ sample} / OD_{(550-650)} \text{ control}) \times 100$. PEI cytotoxicity was also evaluated for comparison purposes by using relative equivalent concentration. Cell cytotoxicity experiments were performed in triplicate.

3. Results and discussion

3.1. Characterization of A–F bolaamphiphiles aqueous dispersions

The objective was to correlate the structure of the bolaamphiphile organizations formed in water by the film method to their ability to complex DNA. Indeed, the shape of clusters formed by the cationic lipids could have an impact on their capacity to complex DNA, so finally on the rate of measured transfection [43–46]. It is well admitted that the lamellarity and/or the fluidity of liposomes influence the transfection rates. It is, therefore, useful to specify the shape of aggregates formed by these bolaamphiphiles in aqueous solutions. In that way, after aqueous dispersions, the sizes of bolas A–F aggregates were characterized by QELS and morphology observations were performed by TEM (Fig. 4). The quality of the dispersion, the size and the morphology of these aggregates in water are reported in Table 1.

For compounds A and B, made of two per-fluorinated segments, light was weakly scattered in water: their aqueous dispersions exhibited very poor stability and precipitated after 15 min. In that case, TEM micrographs clearly showed the formation of vesicles that quickly clustered in the form of tubular structures (Fig. 4a and b). This property of bolaamphiphiles was already evidenced through peptidic [47,48], glycosidic [49,50] or nucleobase [51–54] derivatives. Moreover, some published data reported that the fluorine content had an impact on the tubules formation in water, due to the added rigidity of fluorocarbon chains as compared to the hydrocarbon analogues [55–58]. This effect must be granted priority to explain the associative behavior of compounds A and B.

In that way, replacement of fluorinated chains by hydrocarbon chains (compounds C and D) led to an increase of solubility and dispersion stabilizations. In such case, the formation of vesicles (MLV) (compound D, Fig. 4f) or of monolamellar membrane systems (compound C, Fig. 4c–e) were noted.

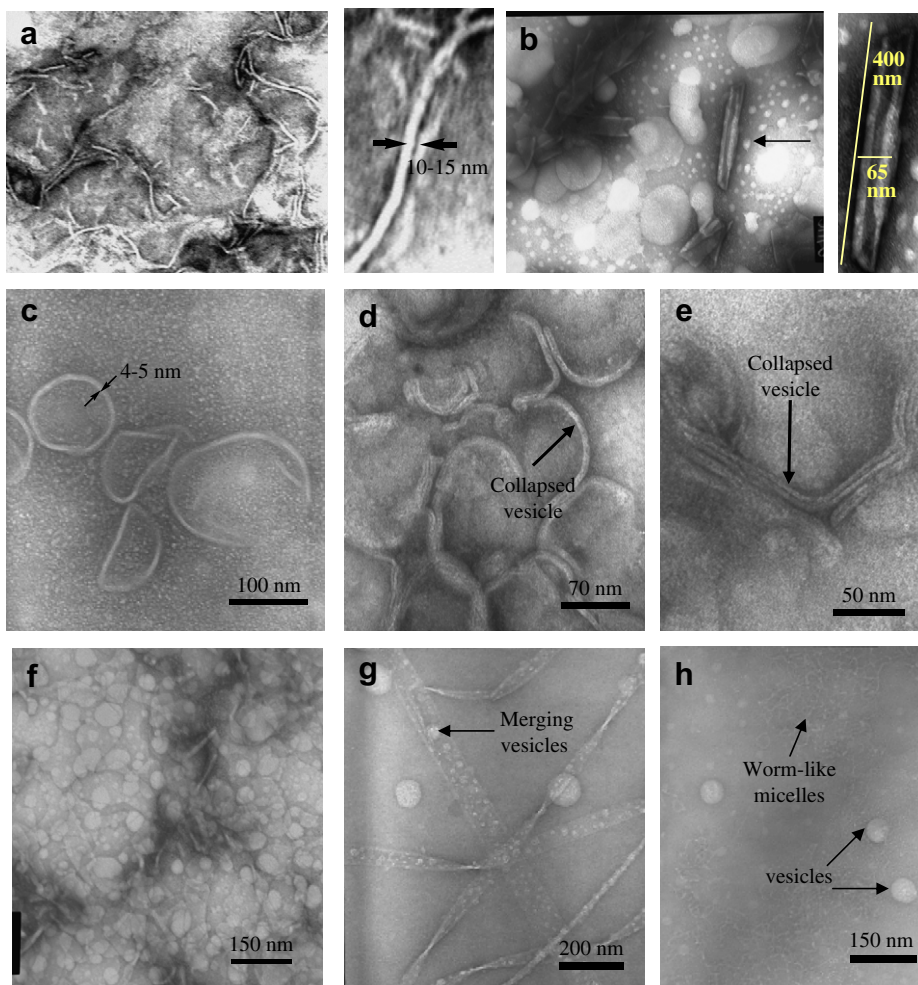


Fig. 4. TEM micrographies of the self-assembled structure formed in water from bolaamphiphiles (a) **A**, (b) **B**, (c–e) **C**, (f) **D**, (g) **E**, (h) **F**.

The nature of cationic polar head groups also influenced the organization capacity of those bolaamphiphiles. Dispersion of bolaamphiphile **C** was indeed easier. Bolaamphiphiles endowed with cationic lysine derived polar head gave much more stable dispersion than their analogues bearing histidine moiety, *i.e.*, an imidazole moiety. To explain such a difference, one can observe that at $\text{pH} = 7$, the imidazole group ($\text{p}K_{\text{a}} = 6$) is only partially protonated and this low ionization can explain its poor dispersibility in aqueous solution (Table 1, entry 4).

Among the four hemifluorinated double stranded bolaamphiphiles, compound **C** seemed to show the best ability leading to stable vesicle dispersions. As confirmed by the results obtained by light scattering, sizes of the vesicles were smaller than 100 nm and polydispersity index was low, pointing to the formation of homogeneous solutions. TEM observations allowed

us to specify the membrane thickness which was in the range of 4–5 nm, *i.e.*, the thickness of lipid bilayers. This suggested a monolamellar organization of bolaamphiphiles (Fig. 4c). Very fluid vesicles tended to collapse under the observation conditions of the TEM. These collapsed vesicles looked like classic membrane systems with lipid bilayers (Fig. 4d and e).

When the perfluorinated segment was replaced by a hydrocarbon segment (compound **E**) or when the side chain was suppressed (compound **F**), the hydrophobic character of the compound is markedly decreased. QELS measurements showed that there were two kinds of supramolecular organization: a major population whose size varied from 13 (compound **E**) to 24 nm (compound **F**) and which should correspond to the formation of large micelles or worm-like micelles detectable by TEM (Fig. 4g and h), next to these micelles, larger aggregates coexisted. Compound

Table 1
Physicochemical properties of bolaamphiphiles A–F

Bolas	Number of fluorinated segments	Dispersibility ^a	Morphology aggregates ^b	Mean particle diameter	
				Volume distribution (nm)	PDI ^c
A	2	Fair	Fibers	73 (73%); 965 (26%)	0.37
B	2	Poor	Vesicles and fibers	404 (100%)	0.32
C	1	Good	Vesicles	90 (100%)	0.26
D	1	Fair	Vesicles and fibers	323 (43%); 1306 (56%)	0.48
E	0	Good	Micelles and fibers	13 (93%); 793 (6%)	0.56
F	1	Good	Micelles and fibers	24 (52%); 157 (47%)	0.22

^a Visual assessment.

^b Studied by TEM.

^c Polydispersity index.

E formed lamellar structures (that can be seen on the ribbons on Fig. 4f) from the fusion of smaller particles, micelles and vesicles. Compound **F** self organized as vesicles, too. The coexistence of micelles and vesicles was likely due to the association under folded of extended shapes of this single thread hemifluorinated compound.

3.2. Study of the complexation of plasmid DNA by agarose gel electrophoresis

The ability of bolaamphiphiles to complex and neutralize plasmid DNA pBudCE4.1/lacZ/CAT (8433 bp) encoding β -galactosidase was investigated by agarose gel electrophoresis. Agarose gel shift assays were performed on bolaplexes A–F formed at different *N/P* ratios (Figs. 5 and 6). Observation of a complete gel retardation of DNA usually indicates that charge neutralization is achieved since agarose gel electrophoresis separates macromolecules according to their charge and size.

Gel electrophoresis demonstrated that all of the bolaamphiphiles were able to neutralize the DNA. However, the proportion of bolaamphiphiles required to immobilize DNA was largely influenced by their chemical structures. Bola **C** was the most efficient double strand hemifluorinated compound since DNA was completely neutralized at a charge ratio close to 1. In contrast, bolaamphiphiles **A**, **B**, and **D** needed to be used at higher *N/P* ratios (1.75, 2.5, and 1.75, respectively) to reach complete DNA neutralization. Bolaamphiphiles with a histidine head group (bolaamphiphiles **B**, **D**) were less efficient and needed higher *N/P* ratios to completely neutralize DNA comparatively to lysine head group-bolaamphiphiles **A** and **C**. This was not surprising, as it has been noted, given that a large proportion of free amines of the

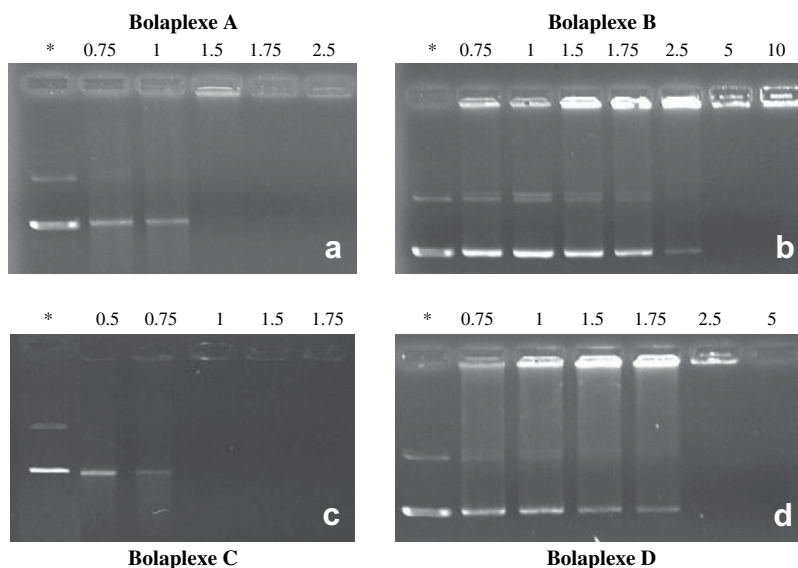


Fig. 5. Representative gel electrophoresis shift assays showing the migration of A–D based bolaplexes formed with pBudCE4.1/LacZ/CAT plasmid. Wells were loaded with an equivalent of 400 ng of DNA. Figures show the migration of bolaplexes formed from bolaamphiphiles: (a) **A**; (b) **B**; (c) **C**; (d) **D**. *N/P* ratios are indicated above the wells. Naked DNA was used as a negative control (*).

imidazole groups was probably not protonated (pK_a close to the physiological pH) under experimental conditions.

The lack of flexibility induced by the presence of a fluorinated chain resulted in less efficient complexation, since these lysine derivatives complexed the plasmid to a higher N/P ratio. The presence of a residual fluorescence in the wells suggests that DNA was not in a highly condensate state. Thus it has to be underlined that a parallel cannot be drawn between the self-associative capacity of those bolaamphiphiles and their DNA complexation efficiency. Notably, the formation of fibrous type organized systems (compounds **A**, **B**, and **D**) was apparently detrimental for efficient plasmid complexation (Fig. 5). Compound **C** that was found clustered in water in fluid bilayers, self-organized more easily with DNA, which entailed N/P load charges very close to 1 when completely complexing DNA.

The absence of a fluorinated segment within the hydrophobic core of the bola (bola **E**) seemed to have strong influence on DNA neutralization and on the condensation process, since higher N/P ratios had to be used (Fig. 6). Again, the presence of notable residual fluorescence in the wells of bolaplex **E** probably indicated a poorly condensed DNA state (Fig. 6a). Single stranded compound **F** complexed the DNA at N/P ratio weaker than 1.75 (Fig. 6b). For the latter, it is worth noting the emergence, at weak N/P ratios, of a spot evidencing higher electrophoretic mobility than supercoiled DNA. This rare phenomenon was also reported by Behr et al. with nanometric DNA particles [59]. Such an observation suggested that a part of the DNA was condensed in small negatively charged particles that probably spread more quickly in the gel than supercoiled DNA.

Moreover, for bolaplex **C**, no residual fluorescence was visible in the well at complete neutralization ($N/P = 1$) in contrast to other lysine head group

bolaamphiphiles. This suggests that structural parameters other than the nature of the charge might influence the interaction of bolaamphiphiles with DNA. The actual physical basis remains to be clearly elucidated.

3.3. Study of the complexation of plasmid DNA by ethidium bromide spectrofluorometric displacement assay

Displacement assays employing a fluorescent dye are commonly used to characterize the interactions between cationic carriers and DNA, in particular to illustrate the state of condensation of DNA in the complexes. It allows for a qualitative comparison of binding affinities within a series of compounds with similar structures [40]. In the present study, an Ethidium Bromide (EtBr) displacement assay was employed to compare the interaction of bolaamphiphiles **A–F** with DNA according to the N/P ratios. The ability of bolaamphiphiles **A–F** to displace EtBr from DNA is shown in Fig. 7. The lower relative fluorescence intensity (I) points out a greater interaction between bola and plasmid DNA. Data showed that as the proportion of bola (N/P ratios) increased for the preparation of bolaplexes, the relative fluorescence intensity (I) of the EtBr/DNA complexes decreased down to a minimum level. The decrease in the fluorescence intensity depended on the N/P ratio utilized and this was distinctive of each bola tested. Data presented in Fig. 7 showed that bolas **A**, **B**, **D** and **E** have similar affinities to DNA since high N/P ratios had to be used to reach 50% inhibition of the initial DNA–EtBr fluorescence (IC_{50}). Even at high N/P ratios DNA intercalation of ethidium bromide was possible. These observations suggested that the affinities of these bolaamphiphiles to DNA were relatively weak.

The IC_{50} values of bolaamphiphiles **C** (1–1.5 N/P ratios) and **F** (1.5 N/P ratio) were smaller than those

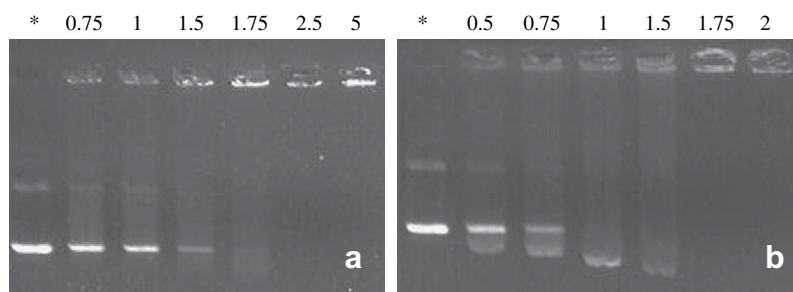


Fig. 6. Representative gel electrophoresis shift assays of bolaamphiphiles (a) **E** and (b) **F** complexed with pBudCE4.1/LacZ/CAT plasmid. Wells were loaded with 400 ng of DNA (1 equiv.). N/P ratios are indicated above the wells. Naked DNA was used as a control (*).

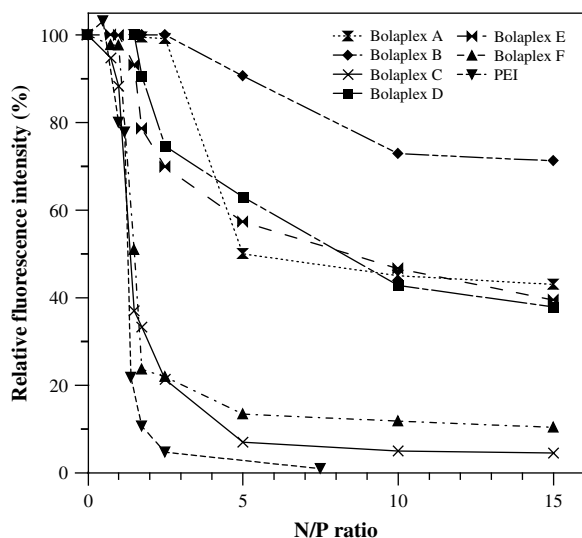


Fig. 7. Ethidium bromide spectrofluorimetric displacement assays. Complexation of DNA plasmid by the bolaamphiphiles was illustrated by the displacement of the fluorescent probe ethidium bromide (EtBr). The relative fluorescence intensity of the resulting complex was expressed by the following equation: Relative fluorescence intensity (I) = $F_{\text{obs}} - F_0 / F_{\text{DNA}} - F_0$; where F_{obs} is the fluorescence intensity of the bolaplexes, F_0 is the fluorescence intensity of the dye in water alone, and F_{DNA} is the dye-labeled DNA in the absence of bola.

calculated for bolaamphiphiles **A** (5), **B** (>30), **D** (>5) and **E** (10) (see Fig. 7). In the case of **C** or **F** bolaplexes (*i.e.*, bolaamphiphiles/DNA complexes), at a ratio N/P of 2.5, the residual fluorescence was almost close to baseline fluorescence ($\sim 20\%$ of the 100% fluorescence associated with the naked DNA–EtBr complex) and to that of PEI bolaplex. Though these data did not offer visualized indications of DNA condensation, they may suggest important morphological changes in DNA structure during its complexation process with **C** or **F** bolaamphiphiles and an affinity to double-helical DNA higher than EtBr (which is usually high and specific). Thus we can assume that structural parameters influence the interactions of **C** or **F** bolaamphiphiles with DNA; at least a cationic head group derived from lysine (or other amine having high pK_a) and a mono-fluorinated main chain seem to be essential for maximal interaction of bola with DNA.

3.4. Stability of A–F bolaplexes to Dnase I treatment

Stability measurements of bolaplexes against DNase I treatment were performed to investigate the degree of protection conferred to DNA when complexed with bolaamphiphiles. Fig. 8 shows DNase I treatments (three replicated studies) of bolaplexes

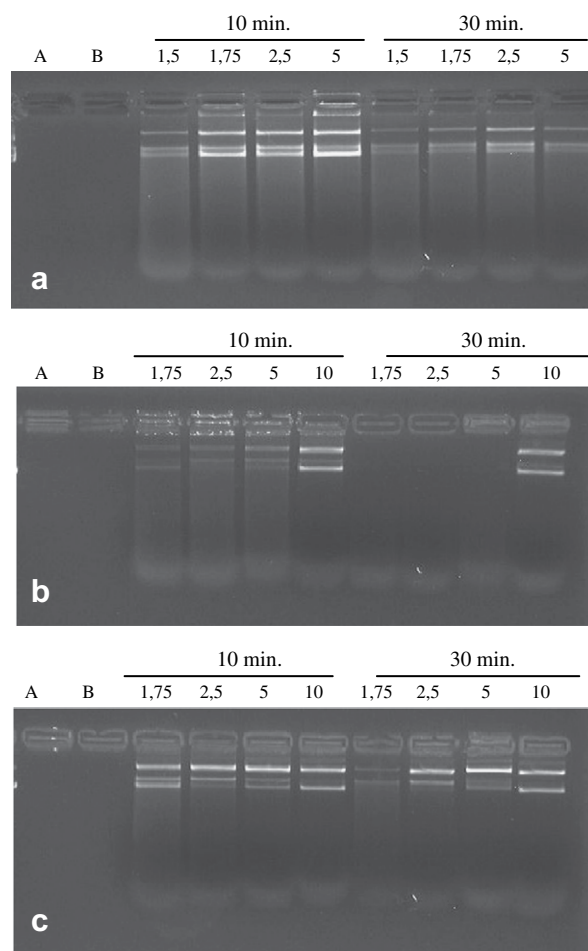


Fig. 8. Stability of bolaplexes against *in vitro* DNase I treatment. DNA degradation was visualized with agarose gel following incubation of bolaplexes over 10 or 30 min with 1 U of DNase I/ μg of DNA. Treatment of (a) bolaplex C; (b) bolaplex E and (c) bolaplex F was reported. Duration of the nuclease treatment and N/P ratios is indicated above the wells. Naked DNA was used as positive control (A, B lanes) of DNase activity.

formed with plasmid DNA and bolaamphiphiles **C**, **E** or **F**. Naked DNA was used as a positive degradation control. Results showed that the level of DNA degradation evolved according to the N/P ratio used and the time of treatment. Well A (naked DNA treatment) showed that, after 10 min incubation, complete DNA degradation had occurred, since no signal was detectable. For **A**, **B**, or **D** bolaplexes, 30 min nuclease treatment resulted in complete degradation of DNA for any N/P ratios tested, except for the highest N/P ratios (data not shown). This observation indicated that DNA complexation with histine head group bolaamphiphiles did not prevent the degradation of plasmid DNA by nucleases. In contrast, DNA complexation with

bolaamphiphiles **C**, **F**, or **E** bearing lysine group offered an effective protection of plasmid DNA.

Following a 10 min DNase I treatment, it is worth noting that the proportion of non-digested DNA seemed to be higher for **C** and **F** bolaplexes. As a higher level of protection was observed for lysine head group-bearing bolaamphiphiles, once again it can be suggested that the nature of the ionic head group is crucial for the DNA protection against nuclease. Moreover, as fluorinated bolaamphiphiles **C** and **F** seemed to confer higher levels of protection compared to the non-fluorinated analogue **E**, it can be still assumed that the fluorinated chain was an important structural parameter implied in the protection of DNA against DNases.

The type and strength of interaction with DNA imposed by the structural characteristics of bolaamphiphiles during complexation could be largely involved in their protection. Indeed, among the bolaamphiphiles and variable *N/P* ratios implemented in this study, no total protection from hydrolysis by DNase I could be observed. Many hypotheses could explain this observation. For instance, DNA could be trapped at the surface of the nanospheres and consequently be more exposed to DNase attacks. An other cause would be that DNA compaction by bolaamphiphiles is not completely achieved due to the limiting amount of cationic charge available.

3.5. Physicochemical characterizations of bolaplexes: size, ζ -potential and transmission electron microscopy

A summary of the particle size and zeta potentials of bolaplexes as measured in water at room temperature is shown in Table 2. It is well known that the size and the surface charge of the complexes play a critical role in gene transfer efficiency [60], complexes greater than 150 nm appearing less capable to be endocytosed by somatic cells [61].

The data presented in Table 2 show that the size of the **A**- and **D**-bolaplexes is modulated by the variation of the *N/P* ratios. Their sizes are small at low *N/P* ratios but tend to increase significantly above this value (≤ 1.5). Both **A**- and **D**-bolaplexes had a negatively charge surface (measured by ζ -potential) at all of the charge ratios, suggesting that charge neutralization did not occur. However, electrophoresis experiments clearly showed DNA complexation at a 2.5 *N/P* ratio, but EtBr displacement as well as resistance to DNase experiments have shown that DNA was not settled under very condensed form. Consequently, it can be assumed that part of the DNA could be immobilized on the outer surface of the bolaplex. For compound **B**, no

Table 2
The ζ -potential and mean diameters of **A–F** bolaplexes

<i>N/P</i>	A		B		C		D		E		F	
	ζ -pot. (mV) ^a	d (nm) ^b	ζ -pot. (mV) ^a	d (nm) ^b	ζ -pot. (mV) ^a	d (nm) ^b	ζ -pot. (mV) ^a	d (nm) ^b	ζ -pot. (mV) ^a	d (nm) ^b	ζ -pot. (mV) ^a	d (nm) ^b
0.75	-22.1 ± 1.5	85 (0.34) ^d	—	—	—	—	—	—	—	—	-43 ± 2.8	— ^c
0.85	—	—	—	—	-37.3 ± 1.9	65 (0.17)	—	—	—	—	—	—
0.9	—	—	—	—	-10.4 ± 1.0	167 (0.21)	—	—	—	—	—	—
1	-30.7 ± 3.8	75 (0.27)	—	—	-14.2 ± 0.1	150 (0.30)	-23.6 ± 0.3	76 (0.35)	-34.9 ± 1.4	324 + 79	-34 ± 4.3	65 (0.32)
1.16	—	—	—	—	28.1 ± 1.4	142 (0.61)	—	—	—	—	—	—
1.29	—	—	—	—	21.5 ± 2.7	85 (0.70)	—	—	—	—	—	—
1.4	—	—	—	—	45 ± 2.4	— ^c	—	—	—	—	—	—
1.5	-34.2 ± 2.7	67 (0.21)	—	—	—	—	—	—	—	—	-25 ± 1.5	84 (0.22)
1.75	-35.4 ± 0.7	115 (0.28)	-31 ± 1	— ^c	57.4 ± 1.3	— ^c	—	—	-28 ± 0.5	500 + 120	-26 ± 1.8	80 (0.26)
2.5	-11 ± 1.5	224 (0.50)	-4.5 ± 1.2	— ^c	—	— ^c	-31.1 ± 0.5	152 (0.33)	— ^c	— ^c	-28 ± 2.2	66 (0.43)
5	—	—	—	—	—	—	-20.1 ± 3.0	218 (0.78)	48 ± 0.7	1200 + 200	36 ± 1.3	81 (0.35)

^a Zeta potential ± SD (mV).

^b Volume distribution.

^c Unstable preparation.

^d Polydispersity index.

size measurement could be obtained due to the marked instability of the bolaplexes in solution. The peculiarity of the three (**A**, **B**, **D**) bolaamphiphiles was their strong hydrophobic character due to either their fluorinated content (compounds **A** and **B**) and/or the presence of imidazole moiety, as DNA complexing group partly protonated at physiological pH (compound **D**). These strong hydrophobic properties were probably the driving force for the aqueous thread-like self-organization of these bolaplexes (Fig. 9). With **A**-bolaplex solutions, TEM evidenced spherical particle formation (Fig. 9a) whose size confirmed data obtained from QELS (100–200 nm for $N/P = 1.75$). **D**-bolaplex solutions are composed of fibrous structures and vesicles (Fig. 9b) detected by QELS as two aggregate populations.

As regards compound **C**, ζ -potential measurement indicated that this bolaamphiphile was able to neutralize the DNA charges. We noted an inversion of ζ -potential to positive values beyond an electric charge ratio higher than 1. It has to be underlined the increase in the particle size when electroneutrality was reached ($N/P = 0.9$ –1). Then, when the charge of **C**-bolaplex became positive ($N/P > 1$), the particle size decreased to reach the lowest value (85 nm) at N/P ratio of 1.29 [39,62].

TEM images clearly showed the presence of small-sized particles with internal lamellar-like order (Fig. 9c–d). Similar ordered structures have already been observed for lipoplexes through electronic microscopy [63–68]. It is worth noting that bola **E** – the fully hydrocarbon analogue of compound **C** – did not form the same type of bolaplex. QELS indicated the emergence of two aggregate populations, one of which is very large and corresponds to the formation of thread-type structures visible in TEM (Fig. 9e). When the N/P ratio increased, the proportion of fibers present in the solution also increased markedly (Fig. 9f). At lower N/P ratio (Fig. 9e), vesicles probably corresponding to the smaller population detected by QELS (80–200 nm) could also be noted. Even when the surface charge of these aggregates was reversed, aggregates size thus formed went on increasing. For $N/P = 2.5$, size and zeta potential measurements indicated the instability of the aggregates formed, which suggest that the charge neutralization ratio is reached. The neutralization of DNA phosphate groups was achieved with N/P ratios higher than those previously measured with compound **C**.

On the other hand, without the hydrocarbon lateral chain, compound **F** formed small self-assembled lamellar bolaplexes (Fig. 8b), namely

smaller than 100 nm [for N/P ratios varying between 1 and 5 and even if surface charge reversal was only achieved for high charges ratios ($N/P = 5$)]. Nevertheless, data obtained with ethidium bromide displacement assays indicated that complete complexation of DNA was reached at the same N/P ratio than compound **C**. The affinity for DNA appeared to be identical but charge reversal was achieved for higher N/P values. TEM images of **F**-bolaplex showed the same regular organization as for **C**-bolaplex (Fig. 9g and h). Therefore, it seems that the formation of self-organized multilamellar systems was closely linked to the hemifluorinated structure of these bolaamphiphiles.

TEM observations (Fig. 4) and QELS studies (Table 1) showed the micellar behavior of compound **F** alone in aqueous solution. This micellar behavior linked with the formation of small-sized aggregates was also evidenced by Pitard and coworkers using lipopolyamine [63]. Micelles are dynamic organization whose life spans are much shorter than membrane systems. Therefore, bolaplex organization becomes virtually independent from the bolaamphiphile initially organized structure if the latter is fluid and reversible. Nevertheless, this lability may become a hindrance to DNA plasmid complexation, as the forces leading to DNA complexation are of electrostatic and hydrophobic origins in the case of bolaplexes organization.

The surface electric charge of bolaplexes formed from compounds **C** and **F** was totally different at a $N/P = 1.75$ ratio. ζ -Potential of **C**-bolaplex equaled +57.4 mV and that of **F**-bolaplex –26 mV. The difference in electric charge behavior between the two bolaplexes might be correlated to the structure of the associations formed before complexation. Compound **C** self-organized as monolayer vesicles (Fig. 4c and e). In that case, it was likely that charge distribution occurred in a statistical manner on either side of the membrane in order to decrease the electrostatics repulsive interactions between polar heads. This metastable monolayer system distributed itself around the DNA to complex it without breaking-up while maintaining its original membrane structure. Such an organization might lead to the formation of sandwich-like lamellar structures whose surface would be covered by cationic and glycosidic polar head groups, so to a net positive surface electric charge (Fig. 10).

As regards **F**-bolaplex, TEM and QELS experiments clearly indicated that this bolaamphiphile self-organized in water as micelle-like systems. In this context, plasmid complexation would be achieved from micelles or free bolaamphiphiles (Fig. 11).

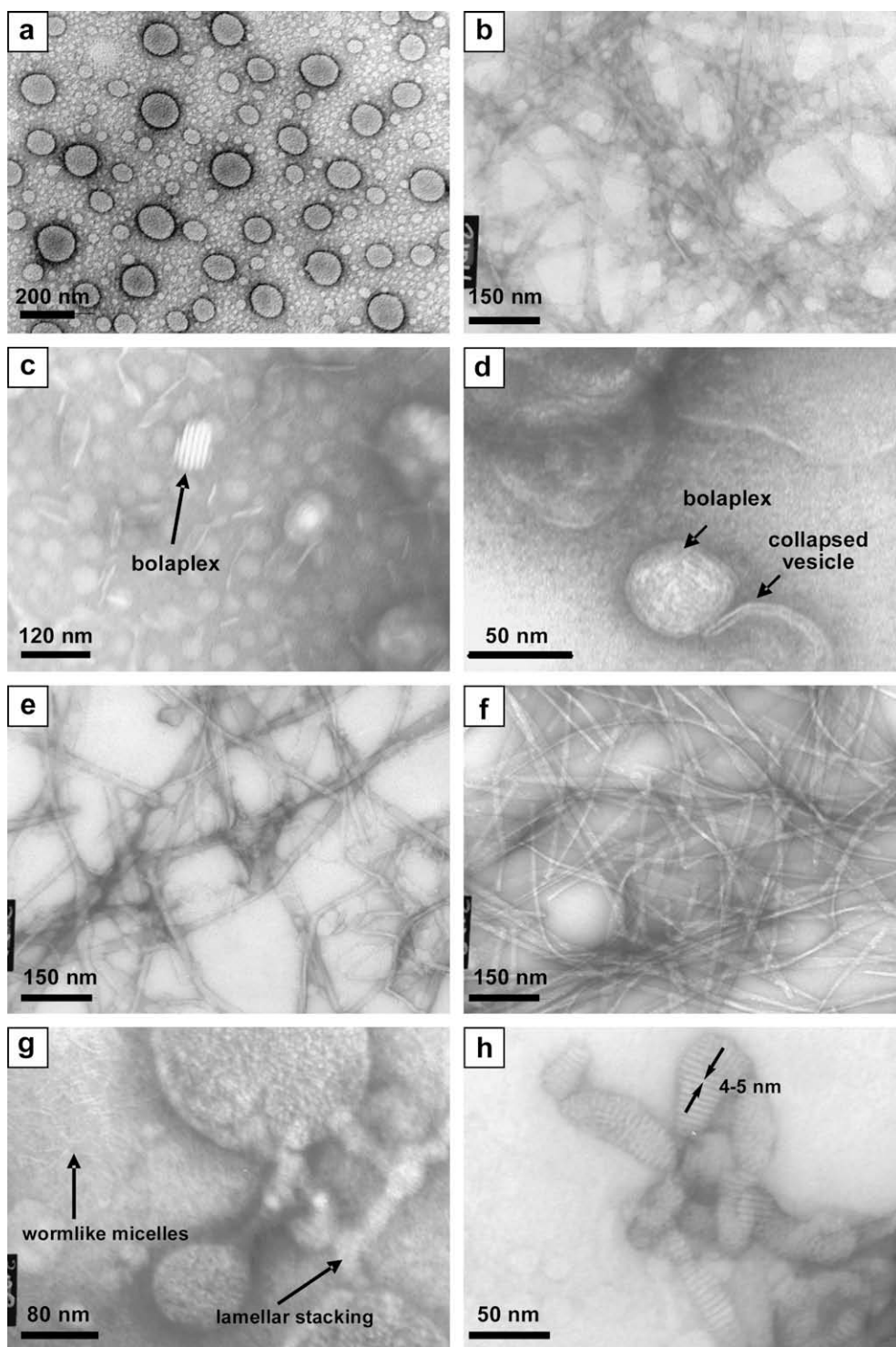


Fig. 9. Representative TEM images showing the morphology of (a) A-bolaplex ($N/P = 1.75$), (b) D-bolaplex ($N/P = 1.75$), (c) C-bolaplex ($N/P = 1.75$), (d) C-bolaplex ($N/P = 5$), (e) E-bolaplex ($N/P = 1.75$), (f) E-bolaplex ($N/P = 5$), (g) F-bolaplex ($N/P = 1$) and (h) F-bolaplex ($N/P = 5$).

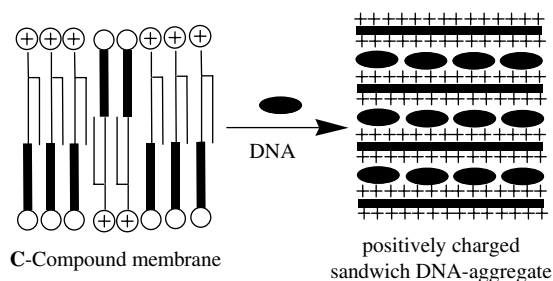


Fig. 10. Lamellar complexation of DNA plasmid by C-bolaamphiphile membranes.

Finally, in Fig. 9h, it has to be underlined that the F-bolaplex ($N/P = 5$ ratio, positive zeta potential) presented a periodic lamellar internal structure with a thickness of 4–5 nm section that was the same as one of the monolamellar membrane formed from bolaamphiphile C (Fig. 4c). Such a result tends to show that, when electroneutrality is reached (for a high N/P ratio), F-bolaplex present a close behavior to C-bolaplex.

3.6. Cell viability studies

The effect of bolaamphiphile and bolaplex amounts on cell viability (metabolic activity) was investigated and is presented in Fig. 12. The relative percentage of cell viability of COS7 cells was firstly reported for varying bolaamphiphile concentrations (calculated in accordance with the different N/P ratios experiments) and, secondly, for different N/P bolaplex ratios (varying between 1 and 10) after a treatment of 24 h. Branched poly(ethylenimine) (PEI) 25 kDa was reported as a standard. PEI is known to be a potent transfectant but with acute cellular cytotoxicity.

The results indicated that bolaamphiphiles A, B, D, F had a moderate toxic effect (much lower than the PEI) on the cell. Cell viability decreased with the increase of bolaamphiphile concentration. As PEI was reported to be less toxic than the lipids [69], we can indirectly conclude that these bolaplexes are less

cytotoxic than other lipid transfectant reagents. Furthermore, we can note that compound F exhibited a higher toxicity than compound C. As we mentioned above, compound F could fold its main chain to self-organize as micelles. This structural and behavior specificities could explain its higher toxicity. Indeed, Fyles et al. showed that membrane disruption mechanism might occur via U-shaped conformation of the bolaamphiphiles [70]. Therefore, the presence of a side chain might prevent the folding and cytotoxicity of those bolaamphiphiles.

3.7. Reporter gene expression in COS-7 cells

In order to evaluate the gene delivery potential of A–F bolaplexes, the *in vitro* transfection efficiency of A–F bolaplexes were performed on COS-7 cell lines. Data corresponding to the different transfection experiments are presented in Fig. 13. A, B, D and E bolaplexes failed to transfect COS-7 cells regardless the N/P ratio used, contrasting with C and F bolaplexes. The difference in the transfection efficiencies observed between C-bolaplex and E-bolaplex might be due, at least in part, to the inability of the non-fluorinated bolaform to bind, protect and condense efficiently DNA. This result suggests that the partial fluorination of the hydrophobic core of these bolaamphiphiles increases not only the self-association and DNA complexation abilities of these compounds but also their DNA transfection efficiency.

Bolaamphiphiles C and F that alone were capable to organize the plasmid in the form of a small-sized multilamellar bolaplex, were also the only ones in a position to efficiently transfect DNA. F-bolaplex offered COS-7 cell transfection rates considerably lower than C-bolaplex, but in both types of bolaplexes, DNA internal organization and condensation rate appeared very close to each other. As the apparent organization of both bolaplexes was virtually identical, there followed that their main discrepancy factor was

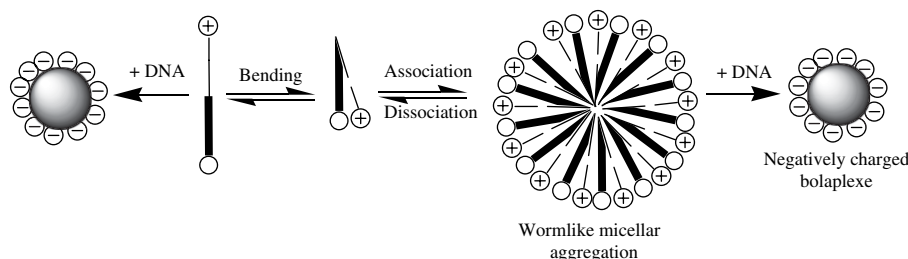


Fig. 11. Complexation of DNA plasmide with F-bolaamphiphile micelles.

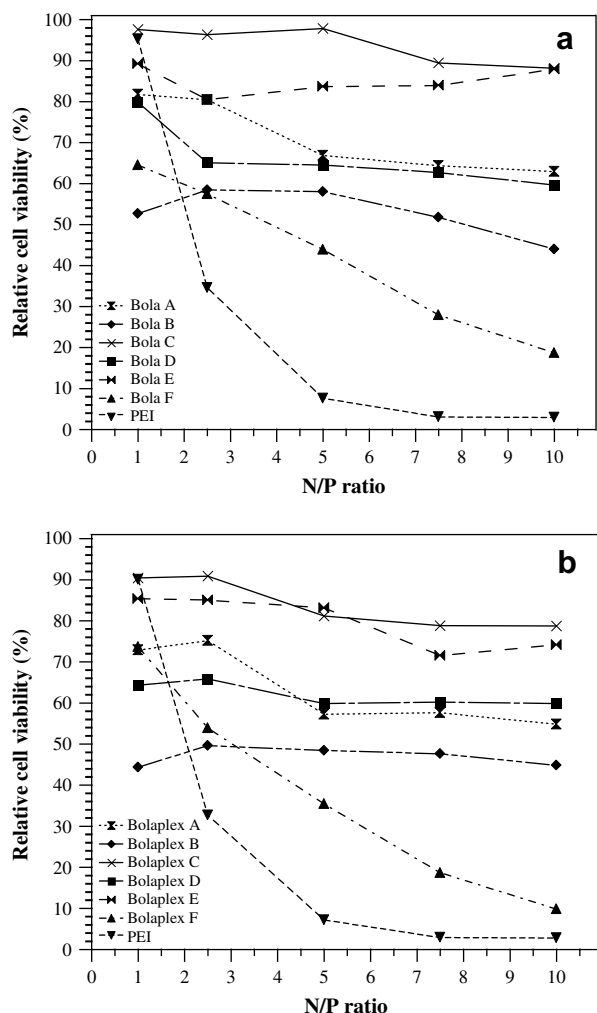


Fig. 12. *In vitro* cells viability of COS7 cells treated with bolaamphiphiles A–F alone (a) and A–F type bolaplexes (b). In the two figures, the relative viability of COS7 cells after a 24-h treatment is expressed as a function of *N/P* ratio.

their surface electric charge at the respective maximal *N/P* ratio – negative for F-bolaplex and positive in the case of type-C bolaplexes. Gene transfer is known to be optimal when particles are positively charged for binding the anionic cell surface of the cells. As reported elsewhere [67,71,72], the decrease in transfection efficacy for F-bolaplex could be related to the repulsive interaction between negative surface charge of bolaplexes and the negative charge of the plasma membrane. C-bolaplex generated a significant transfection level, presenting a bell-shaped profile and a maximum level of transfection at a *N/P* ratio of 1.5, typically higher than three orders of magnitude than naked DNA of the same order of magnitude as that generated by PEI polyplexes (*N/P* = 10). Therefore,

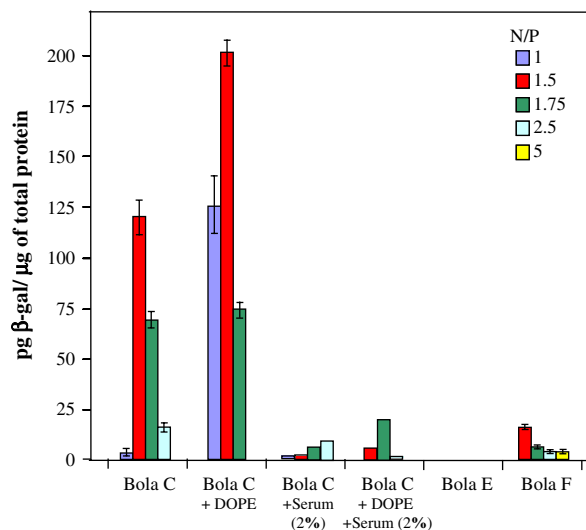


Fig. 13. Transfection efficiency of the plasmid pBudCE4.1/lacZ/CAT complexed with bola C, C/DOPE, E or F (prepared by using *N/P* ratios in the range of 1–5) in the presence or not of serum using the COS7 cell line. Results were expressed as the picogram concentration of β-galactosidase/μg of total protein.

C-bolaplexes are efficient transfection reagents with relatively low cytotoxicity comparatively to the PEI.

3.8. Transfection with DOPE-based complexes

DNA affinity and complexation process reversibility appeared to be important factors allowing lipofection efficacy. Other teams showed effectively that existence of strong binding interactions between DNA and the cationic liposome or polymer induce poor gene transfer efficacies [12,44,46,73–75]. On the other hand, following the hypothesis that structural organization within lipoplexe would have a considerable impact on lipofection [44], Zuhorn and coworkers showed that the presence of DOPE in SAINT-containing lipoplexes induced a less effective packaging of the DNA [73]. According to these observations, DOPE was introduced in C-bolaplex formation in order to increase the transfection efficiency of bola C. Higher transfection levels were measured by the addition of DOPE in bolaplexes formation comparatively to the original C-bolaplex (see Fig. 13). Notably at small *N/P* ratios (*N/P* = 1 and 1.5), the presence of DOPE dramatically increases (40×) the transfection efficiency of the bolaamphiphile C.

Thus, the existence of structural defects within lipoplexe organization might optimize lipofection [44]. According to this hypothesis, by most likely

introducing bolaplex disruption, DOPE use (as a helper lipid) would allow an increase in bolaplex lipofection capacity. Zuhorn et al. showed that DOPE incorporated to lipoplexes induced a less effective packaging of the DNA as reflected by an enhancement in accessibility of the plasmid for labelling with picogreen [73].

3.9. Transfection in presence of serum

C, E, F and C-DOPE bolaplexes were also tested for their *in vitro* transfection efficiency in the presence of 2.0% serum. Data are presented in Fig. 13. It is shown that transfection efficiency with C and C-DOPE bolaplexes decreased drastically in the presence of serum. The presence of serum completely inhibited the low transfection capacity of bolas E and F (data not shown). Moreover, in spite of higher transfection level observed for bola C-DOPE (compared to C-bolaplex), the presence of co-lipid helper seems not to help the transfection in the presence of serum. The decrease in the transfection efficiency in the presence of serum suggests that the stability/integrity of bolaplexes is greatly disturbed in such situation. It illustrates a weak interaction between bolaamphiphile and DNA that facilitated the precocity of decomplexation of bolaplexes in the presence of serum. The anionic and cationic species present in the serum appear to be detrimental for the stability of the bolaplexes. In addition, the decrease in transfection efficiency can be attributed to the poor resistance to DNases present in the serum. Finally, the positive charge of the bola C based complexes have an effective negative impact on the transfection level in the presence of serum; the interactions with negatively charged proteins weaken DNA complexation, allowing access to DNases. However, other factors than the charge surface seem to influence the transfection efficiency in the presence of serum since transfection with negatively charged F-bolaplex has a reduced efficiency. Complex instability could be the main factor related transfection efficiency decrease in the presence of serum.

4. Conclusions

A new series of dissymmetric hemifluorocarbon bolaamphiphiles were evaluated for DNA complexation as well as *in vitro* gene transfer carrier. Bolaamphiphiles organized in a bilayer form allowed for an efficient complexation and condensation of DNA. The chemical structure of the bolaamphiphiles affected the DNA condensation. Bolaamphiphiles with lysine head groups were much prone to neutralize and condense

DNA than their analogues with histidine groups. The incorporation of two fluorinated segments in the molecular structure of the bolaamphiphiles is detrimental for an efficient DNA condensation. In contrast, a partial fluorination of the hydrophobic core of bolas increased not only the DNA complexation abilities but also the DNA transfection efficiency. Relatively high transfection activity was obtained for the bolaamphiphile possessing a lysine head-group and one fluorinated segment close to the carbohydrate moiety. This result could be explained by the small size and the positive surface charge of the bolaplex. However, this positive charge has a negative impact on the transfection level in the presence of serum; the interactions with negatively charged proteins decrease DNA complexation and the transfection efficiency of such compounds as already noted with various lipoplexes. According to this hypothesis, work is currently undertaken to prepare new dissymmetric fluorinated bolaamphiphiles leading to small bolaplexes showing a very low electric charge on their outer surface.

Acknowledgements

This work was in part supported by Valorisation Recherche Québec (Gouvernement du Québec, Project Number: 2201-141) and by the Ministère de l'Enseignement Supérieur et de la Recherche Français which provided a grant to Ph.D. student Séverine Denoyelle. We are thankful to Diane Montpetit for her invaluable help in conducting examination by transmission electronic microscopy, Professor René Roy (UQAM, Québec) for his valuable suggestions and councils, Horiba group, Jobin Yvon Spex, fluorescence spectrometer.

References

- [1] V.V. Kumar, R.S. Singh, A. Chaudhuri, *Curr. Med. Chem.* 10 (2003) 1297 and the references therein.
- [2] A.D. Miller, *Angew. Chem., Int. Ed.* 37 (1998) 1768 and the references therein.
- [3] P.L. Felgner, T.R. Gadek, M. Holm, R. Roman, W. Chan, M. Wenz, J.P. Northrop, G.M. Ringold, M. Danielsen, *Proc. Natl. Acad. Sci. U.S.A.* 84 (1987) 7413.
- [4] A. Bajaj, P. Kondiah, S. Bhattacharya, *J. Med. Chem.* 50 (2007) 2432.
- [5] M.N. Antipina, M. Schulze, B. Dobner, A. Langner, G. Brezesinski, *Langmuir* 23 (2007) 3919.
- [6] J. Leblond, N. Mignet, C. Largeau, M.-V. Spanedda, J. Seguin, D. Scherman, J. Herscovici, *Bioconjugate Chem.* 18 (2007) 484.
- [7] V. Gopal, T.K. Prasad, N.M. Rao, M. Takafuji, M.M. Rahman, H. Ihara, *Bioconjugate Chem.* 17 (2006) 1530.

- [8] K.K. Ewert, H.M. Evans, N.F. Bouxsein, C.R. Safinya, *Bioconjugate Chem.* 17 (2006) 877.
- [9] M.A. Iliés, W.A. Seitz, B.H. Johnson, E.L. Ezell, A.L. Miller, E.B. Thompson, A.T. Balaban, *J. Med. Chem.* 49 (2006) 3872.
- [10] P.P. Karmali, B.K. Majeti, B. Sreedhar, A. Chaudhuri, *Bioconjugate Chem.* 17 (2006) 159.
- [11] E. Picquet, K. Le Ny, P. Delépine, T. Montier, J.-J. Yaouanc, D. Cartier, H. des Abbayes, C. Férec, J.-C. Clément, *Bioconjugate Chem.* 16 (2005) 1051.
- [12] J. Sen, A. Chaudhuri, *Bioconjugate Chem.* 16 (2005) 903 and references therein.
- [13] P. Chabaud, M. Camplo, D. Payet, G. Serin, L. Moreau, P. Barthélémy, M.W. Grinstaff, *Bioconjugate Chem.* 17 (2006) 466.
- [14] M. Belting, S. Sandgren, A. Wittrup, *Adv. Drug Deliv. Rev.* 57 (2005) 505.
- [15] K. Kostarelos, A.D. Miller, *Chem. Soc. Rev.* 34 (2005) 970.
- [16] J.H. Fuhrhop, T. Wang, *Chem. Rev.* 104 (2004) 2901.
- [17] J. Guilbot, T. Benvegny, N. Legros, D. Plusquellec, J.-C. Dedieu, A. Gullik, *Langmuir* 17 (2001) 613.
- [18] O. Zelphati, L.S. Uyechi, L.G. Barron, F.C. Szoka, *Biochim. Biophys. Acta* 1390 (1998) 119.
- [19] I. Moret, J.E. Peris, V.M. Guillem, M. Benet, F. Revert, F. Dasi, A. Crespo, S.F. Alino, *J. Controlled Release* 76 (2001) 169.
- [20] D.L. Reimer, S. Kong, M. Monck, J. Wyles, P. Tam, E.K. Wasan, M.B. Bally, *J. Pharmacol. Exp. Ther.* 289 (1999) 807.
- [21] D.M.L. Morgan, V.L. Larvin, J.D. Pearson, *J. Cell Sci.* 94 (1989) 553.
- [22] I.R.C. Hill, M.C. Garnett, F. Bignotti, S.S. Davis, *Biochim. Biophys. Acta* 1427 (1999) 161 (see references therein).
- [23] J.D. Toussignant, A.K. Gates, L.A. Ingram, C.L. Johnson, J.B. Nietupski, S.H. Cheng, S.J. Eastman, R.K. Scheule, *Hum. Gene Ther.* 11 (2000) 2493.
- [24] S. Loisel, C. Le Gall, L. Doucet, C. Férec, V. Floch, *Hum. Gene Ther.* 12 (2001) 685.
- [25] M.A.W. Eaton, T.S. Baker, C.F. Caterall, K. Crook, G.S. Macaulay, B. Mason, T.J. Norman, D. Parker, J.J.B. Perry, R.J. Taylor, A. Turner, A.N. Weir, *Angew. Chem., Int. Ed.* 39 (2000) 4063.
- [26] V. Weissig, V.P. Torchilin, *Adv. Drug Deliv. Rev.* 49 (2001) 127.
- [27] T. Yoshimura, S. Hasegawa, N. Hirashima, M. Nakanishi, T. Ohwada, *Bioorg. Med. Chem. Lett.* 11 (2001) 2897.
- [28] T. Ren, G. Zhang, D. Liu, *Tetrahedron Lett.* 42 (2001) 1007.
- [29] T. Ren, G. Zhang, D. Liu, *Bioorg. Med. Chem. Lett.* 9 (2001) 2969.
- [30] J. Gaucheron, C. Santaella, P. Vierling, *Bioconjugate Chem.* 12 (2001) 569.
- [31] K. Fabio, J. Gaucheron, C. Di Giorgio, P. Vierling, *Bioconjugate Chem.* 14 (2003) 358.
- [32] M.-L. Miramon, N. Mignet, J. Herscovici, *J. Org. Chem.* 69 (2004) 6949.
- [33] S. Denoyelle, A. Polidori, M. Brunelle, P.Y. Vuillaume, S. Laurent, Y. El Azhary, B. Pucci, *New J. Chem.* 30 (2006) 629.
- [34] E. Kissa, *Fluorinated Surfactants. Synthesis, Properties, Applications. Surfactants Sciences Series 50*, Marcel Dekker, New York, 1994.
- [35] M. Kadi, P. Hanson, M. Almgren, *Langmuir* 18 (2002) 9243.
- [36] P. Barthelemy, V. Tomao, J. Selb, Y. Chaudier, B. Pucci, *Langmuir* 18 (2002) 2557.
- [37] K. Liang, Y. Hui, *J. Am. Chem. Soc.* 114 (1992) 6588.
- [38] P.Y. Vuillaume, M. Brunelle, M.R. Van Calsteren, S. Laurent-Lewandowski, A. Bégin, R. Lewandowski, B.G. Talbot, Y. El Azhary, *Biomacromolecules* 6 (2005) 1769.
- [39] V.A. Izumrudov, M.V. Zhiryakova, A.A. Goulko, *Langmuir* 18 (2002) 10348.
- [40] H. Gershon, R. Ghirlando, S.B. Guttman, A. Minsky, *Biochemistry* 32 (1993) 7143.
- [41] O. Boussif, F. Lezoualch, M.A. Zanta, M.D. Mergny, D. Scherman, B. Demeneix, J.P. Behr, *Proc. Natl. Acad. Sci. U.S.A.* 92 (1995) 7297.
- [42] H. Faneca, S. Simões, M.C. Pedroso de Lima, *Biochim. Biophys. Acta* 1567 (2002) 23.
- [43] M.A. Wolfert, P.R. Dash, O. Nazarova, D. Oupicky, L.W. Seymour, S. Smart, J. Strohm, K. Ulbrich, *Bioconjugate Chem.* 10 (1999) 993.
- [44] N.J. Zuidam, D. Hirsch-Lerner, S. Margulies, Y. Barenholz, *Biochim. Biophys. Acta* 1419 (1999) 207.
- [45] A. Ito, R. Miyazoe, J. Mitoma, T. Akao, T. Osaki, T. Kunitake, *Biochem. Int.* 22 (1990) 235.
- [46] T. Akao, A. Ito, *J. Chem. Soc., Perkin Trans. 2* (1997) 213.
- [47] M. Kogiso, S. Ohnishi, K. Yase, M. Masuda, T. Shimizu, *Langmuir* 14 (1998) 4978.
- [48] M. Kogiso, T. Hanada, K. Yase, T. Shimizu, *Chem. Commun.* (1998) 1791.
- [49] T. Shimizu, M. Masuda, *J. Am. Chem. Soc.* 119 (1997) 2812.
- [50] I. Nakazawa, M. Masuda, Y. Okada, T. Hanada, K. Yase, M. Asai, T. Shimizu, *Langmuir* 15 (1999) 4757.
- [51] M. Masuda, T. Shimizu, *Langmuir* 20 (2004) 5969.
- [52] T. Shimizu, R. Iwaura, M. Masuda, T. Hanada, K. Yase, *J. Am. Chem. Soc.* 123 (2001) 5947.
- [53] R. Iwaura, K. Yoshida, M. Masuda, K. Yase, T. Shimizu, *Chem. Mater.* 14 (2002) 3047.
- [54] R. Iwaura, K. Yoshida, M. Masuda, M. Ohnishi-Kameyama, M. Yoshida, T. Shimizu, *Angew. Chem., Int. Ed.* 42 (2003) 1009.
- [55] L. Zarif, T. Gulik-Krzywicki, J.G. Riess, B. Pucci, C. Guedj, A.A. Pavia, *Colloids Surf. A* 84 (1996) 107.
- [56] F. Giulieri, M.-P. Krafft, J.G. Riess, *Angew. Chem., Int. Ed. Eng.* 33 (1994) 1514.
- [57] F. Giulieri, F. Guillod, J. Greiner, M.-P. Krafft, J.G. Riess, *Chem.—Eur. J.* 2 (1996) 1335.
- [58] F. Giulieri, M.-P. Krafft, *J. Colloid Interface Sci.* 258 (2003) 335.
- [59] E. Dauty, J.-S. Remy, G. Zuber, J.-P. Behr, *Bioconjugate Chem.* 13 (2002) 831.
- [60] A.D. Miller, *Methods Mol. Med.* 90 (2004) 107.
- [61] C.W. Pouton, L.W. Seymour, *Adv. Drug Deliv. Rev.* 34 (1998) 3.
- [62] Y. Zhang, T.J. Anchordoquy, *Biochim. Biophys. Acta* 1663 (2004) 143.
- [63] B. Pitard, O. Aguerre, M. Airiau, A.-M. Lachagès, T. Boukhnikachvili, G. Byk, C. Dubertret, C. Herviou, D. Scherman, J.-F. Mayaux, J. Crouzet, *Proc. Natl. Acad. Sci. U.S.A.* 94 (1997) 14412.
- [64] L. Cui, L. Zhu, *Langmuir* 22 (2006) 5982.
- [65] J. Smisterova, A. Wagenaar, M.C.A. Stuart, E. Polushkin, G. ten Brinke, R. Hulst, J.B. Engberts, D. Hoekstra, *J. Biol. Chem.* 276 (2001) 47615.
- [66] B.K. Majeti, P.P. Karmali, S.S. Madhavendra, A. Chaudhuri, *Bioconjugate Chem.* 16 (2005) 676.
- [67] T. Blessing, J.-S. Remy, J.-P. Behr, *Proc. Natl. Acad. Sci. U.S.A.* 95 (1998) 1427.
- [68] E. Dauty, J.-S. Remy, T. Blessing, J.-P. Behr, *J. Am. Chem. Soc.* 123 (2001) 9227.

- [69] C.L. Gebhart, A.V. Kabanov, *J. Controlled Release* 73 (2001) 401.
- [70] T.M. Fyles, B. Zeng, *J. Org. Chem.* 63 (1998) 8337.
- [71] A. Salvati, L. Ciani, S. Ristori, G. Martini, A. Masi, A. Arcangeli, *Biophys. J.* 121 (2006) 21.
- [72] K.A. Mislick, J.D. Baldeschwieler, *Proc. Natl. Acad. Sci. U.S.A.* 93 (1996) 12349.
- [73] I.S. Zuhorn, V. Oberle, W.H. Visser, J.B.F.N. Engberts, U. Bakowsky, E. Polushkin, D. Hoekstra, *Biophys. J.* 83 (2002) 2096.
- [74] D. Hirsch-Lerner, M. Zhang, H. Eliyahu, M.E. Ferrari, C.J. Wheeler, Y. Barenholz, *Biochim. Biophys. Acta* 1714 (2005) 71.
- [75] I. Honoré, S. Grosse, N. Frison, F. Favatier, M. Monsigny, I. Fajac, *J. Controlled Release* 107 (2005) 537.